Nuclear Instruments and Methods in Physics Research B 376 (2016) 116–119

Contents lists available at ScienceDirect

Nuclear Instruments and Methods in Physics Research B

journal homepage: www.elsevier.com/locate/nimb

Design of a single magnet separator with mass resolving power $\frac{m}{\Delta m} \approx 20,000$

Martin Breitenfeldt [a,b,c,*], Mathieu Augustin [b], Richard Catherall [b], Tim Giles [b], Daniel Schoerling [b], Gry M. Tveten [d]

[a] Institut für Physik, Ernst-Moritz-Arndt-Universität Greifswald, Felix-Hausdorff-Str. 8, 17489 Greifswald, Germany
[b] CERN, Route de Meyrin 385, 1217 Meyrin, Switzerland
[c] Avenida Séneca, 2, 28040 Madrid, Spain
[d] Department of Physics, University of Oslo, NO-0316 Oslo, Norway

ARTICLE INFO

Article history:
Received 7 September 2015
Received in revised form 29 January 2016
Accepted 3 February 2016
Available online 2 March 2016

Keywords:
Separator
RIB
Beams
Ion optics

ABSTRACT

ISOLDE at CERN is a leading radioactive ion beam facility. With its upgrade, the HIE-ISOLDE project, an increase in primary beam intensity and energy is envisaged and the aim is a significant increase in intensity of the exotic beams. The high resolution separator (HRS) after the upgrade is required to suppress contaminations almost completely when the masses differ to the beam of interest by $\Delta m/m > 1/20,000$. Here a 120° magnet with a bending radius of 1.25 m has been chosen. The magnetic rigidity is 0.625 Tm (B-field of 0.5 T) to allow for separation of molecules of up to a mass of 300 u. The magnet comprises a yoke in wedged H-type configuration for stability and precision and pole face conductors for focusing and compensation of aberrations. The concept was derived analytically, refined with the OPERA 2D software and tested with the ray-tracing module of OPERA 3D.

1. Introduction

In the ongoing HIE-ISOLDE upgrade an increase in primary beam intensity and energy is envisaged, as well as improved beam quality. These improvements will open the door to new experimental possibilities, but also new challenges related to mass separation. These challenges include radiation protection concerns as well as requiring better beam separation before sending the beam out of the separation zone for improved contamination suppression. The solution is to upgrade the ISOLDE high resolution separator (HRS) which currently has a mass resolving power of $R = \frac{m}{\Delta m} \approx 3000$ for almost 100% suppression of an ion-of-interest to contamination ratio of 1:10^5 and a transmission of 90%. At the moment it hosts the S-shaped separator consisting of a 60° and a 90° magnet. The 90° magnet is equipped with pole face windings to apply corrections to correct transverse aberrations induced by the dipole. Unfortunately their design has underestimated the effect of the yoke for the creation of the correction field. Thus it was never possible to achieve higher mass resolving powers of $R > 11,000$, and also thus limited its intended use to only the lowest masses without significant transmission losses [1]. The design goal of the HRS upgrade is to achieve a mass resolving power of about $R = \frac{m}{\Delta m} \approx 20,000$. A small source emittance is crucial for achieving high mass resolution, and therefore beam cooling is needed before the high resolution stage [2]. The preferred design includes three main components: first a magnetic pre-separator with a small mass resolving power $R \approx 100$ to achieve high isotopic separation, then followed by a radio frequency quadrupole (RFQ) beam cooler to reduce the emittance from the ISOLDE source to a transverse value of $\epsilon_{rad} < 3\pi \cdot \mathrm{mm} \cdot \mathrm{mrad}$ and a longitudinal value of $\epsilon_{axial} < 1$ eV (conservative estimate) [3]. Finally comes the actual separator consisting of electrostatic quadrupole lenses for matching to the dipole magnet. Fig. 1 shows the layout and boundary conditions such as available space. The layout was worked out using the COSY 9.1 beam physics package [4]. The COSY design parameters are given in Table 1 on the upper segment. The second segment of the table gives the correction coefficients required to achieve the desired mass resolution.

2. Design of the magnet

The width of the beam of ± 15 cm dictates a minimum of 30 cm pole width due to the pole overhang, which is required to obtain the relative field uniformity of $5 \cdot 10^{-5}$. In the unoptimized case (no pole face modification) 2.7 times the pole height on each side

* Corresponding author at: CERN, Route de Meyrin 385, 1217 Meyrin, Switzerland.

http://dx.doi.org/10.1016/j.nimb.2016.02.015
0168-583X/

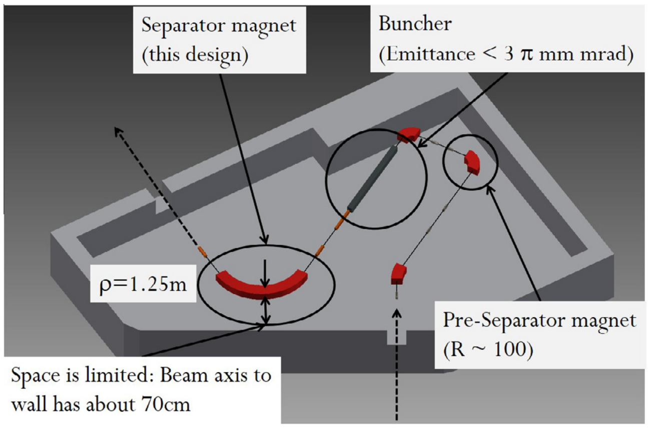

Fig. 1. The new layout designed in the mass separation room. The unseparated beam is entering from the bottom passing through a magnetic pre-separator and its emittance is adjusted in the RFQ cooler before entering the actual separator stage consisting of beam optics and the separator magnet.

Table 1
Design parameters for the 120° magnet as of Ref. [9]. See the text for details.

Beam energy	60 keV
Maximum mass over charge	300 u/e
Magnetic rigidity $B\rho_0$	0.6125 Tm
Bending radius ρ_0	1.25 m
Maximum field B	0.49 T
Bending angle ϕ	120°
Beam width in center of magnet	±15 cm
Quadrupole coefficient α	0.25
Hexapole coefficient β	4.32×10^{-2}
Octupole coefficient γ	8.4×10^{-3}
Pole face width	70 cm
Pole face gap	18 cm

of the good field region is required [5]. Nevertheless, as we are designing for pole face corrections to produce higher order correction terms [6], the shimming of the pole face overhang was omitted, as the relative excitation of the shims can change as function of total magnetic field due to saturation. Last of the design consideration on the pole is the fringe field along the beam axis. In order to have the correct magnetic length the entrance of the magnet is modified with Rogowski profiles [7,8]. Investigation of the robustness of the beamline design with respect to source instability was discussed in Ref. [9]. Furthermore a study of the influence of possible misalignments and voltage jitters is ongoing.

The next step is a transformation of the design parameters into a design of an actual magnet, meaning a yoke and the coils. Very early it has been decided to use pole face conductors to produce the higher order correction terms [6]. This has been tested using the OPERA software [10], which is a finite-element program calculating fields in 2 or 3 dimensions. The first step was the implementation of a yoke, the main coil and the pole face conductors into the 2D version as it less resource intensive. The dimensions of the yoke has been checked and the possibility of the creation of the radial higher field components α, β and γ as described in the equation for the radial dependence of the magnetic field

$$B(\rho) = B_0\left(1 - \alpha\frac{\rho}{\rho - \rho_0} + \beta\frac{\rho^2}{(\rho - \rho_0)^2} - \gamma\frac{(\rho)^3}{(\rho - \rho_0)^3}\right), \quad (1)$$

with B_0 the magnetic field at the reference trajectory of the bending radius $\rho_0 = 1.25$ m. The integrated optimizer of OPERA 2D has been used to evaluate, if the field in the symmetry plane is deviating on average less than 1/20,000. It could be confirmed for an ideal geometry.

As the dipole component of the magnetic field B in the presented geometry is a function of the aperture gap between the poles h

$$B = \frac{2NI\eta\mu_0}{h} \quad (2)$$

with NI being the ampere turns of the coil and η an efficiency factor, irregularities in machining the pole surfaces can have a significant impact on the precision of the magnetic field.

In the case of our design with a pole face separation of 18 cm it would require surface precision of less than 10 μm. This seems very challenging for a magnet of a magnetic length of about 2 m and of a width of about 70 cm. Therefore worst case Monte Carlo analysis has been performed using OPERA 2D simulations. For this analysis the pole face was divided into 10 segments. The corners of the segments horizontal position was varied using the build-in random number generator, create a gaussian distribution with the width of the assumed machining tolerance and 1000 models have been calculated. The field on the symmetry plane was read out on 351 points in the good field region and fitted with Eq. (1) to extract the parameters B_0, α, β and γ for the respective model. The results were plotted as histograms and the extracted FWHM are shown in Table 2 for the case of the dipole component B_0. The precision scales as expected with the machining precision and inverse to the pole face gap, h. The next step involves developing a model, which takes into account the highly 3D nature of this separator magnet due to its large dimensions. The first requirement is the construction of a return yoke, which allows the full operation range of 0.05 T to 0.5 T, and also fits into the separator room and while maintaining the required stability. Here an H-type yoke has been selected. In addition at the entrance and the exit of the magnet an additional 40 cm of iron has been allotted to compensate for the missing volume of return yoke.

Next the entrance and exit of the magnet have been modified to resemble Rogowski profiles [7] for a good mass scalability of the magnet. Nevertheless using the textbook prescription results in a longer field integral than required, which in turn has to be corrected for by offsetting the pole entrance, as discussed below.

The pole face conductors were implemented with the returns outside the yoke to reduce their influence on the outermost trajectories. In the later version 16 pairs of conductors are used with 16 independent currents to create a current distribution of

$$\begin{aligned} I_{pole}(\rho_c) = \; & I_{quad} + I_{hexa}\frac{\rho_c-\rho_0}{w_{pole}} \\ & + I_{octo}\frac{(\rho_c-\rho_0)^2}{w_{pole}^2} + I_{deca}\frac{(\rho_c-\rho_0)^3}{w_{pole}^3} \end{aligned} \quad (3)$$

where ρ_c denotes the radius of the center of the conductor, and for normalization to the maximal value w_{pole} is the width of pole face conductor set. The currents I_{quad}, I_{hexa}, and I_{octo} are required to setup the correction coefficients α, β, and γ from Eq. 1, respectively. Ideally they would be independent, but there is a small contribution from each current to the other components including the dipole B_0. The current I_{deca} is used to reduce the influence of the field line escape towards the side. The design of the 120° magnet is shown in Fig. 2.

Table 2
Precision of dipole component of the magnetic field and its variation for different pole face gap sizes and machining precisions.

Pole gap h (cm)	precision machining (μm)	B_0/T
6	50	0.49(4.3e-4)
6	5	0.49(4.3e-5)
18	50	0.49(1.3e-4)
18	5	0.49(1.3e-5)